Nano Science and Nano Technology

An Indian Journal

Trade Science Inc.

➤ *Full Paper*

Synthesis and textural properties of nanoporous silica with tunable pore size using economic novel linear alkylbenzene sulphonic acid

Mohamed A.Betiha[1]*, Essam M.Ezzo[2], Mohamed F.Menoufy[1], Maged S.Ghattas[1], Ahmad A.Al-Sabagh[1]
[1]Egyptian Petroleum Research Institute, Cairo 11727, Nasr City, P.O. Box 9540, (EGYPT)
[2]Chemistry Department, Faculty of Women for Art, Science and Education, Ain Shams University, (EGYPT)
E-mail : Mohamed_betiha@yahoo.com

ABSTRACT

Large-pore mesoporous silica with 3D wormhole framework structures (denoted as MFG) were prepared through S-I+ assembly pathway from teraethylorthosilicate (TEOS) as the silica source and inexpensive commercially available alkylbenzene sulphonic acid (LASH) as structure-directing agent. The structure and basic properties of the obtained materials were well characterized by various approaches. The results showed that textural porosity of the disordered structures was correlated with the concentration of the surfactant in water. The calcined mesostructures exhibited large pore sizes (3-12.7 nm), surface areas (387–525 m2/g) and pore volumes (0.32–1.76 cm3/g), depending on the surfactant concentration. The textural properties of MFG, wormhole mesostructures, are comparable to those of hexagonal SBA-15 derivatives and large pore MCM-48. However, unlike the SBA-15 structure type, wherein the 3D pore network is formed by connecting 1D cylindrical mesopores through micropores, MFG mesophases have wormhole framework structures containing fully interconnected 3D mesopores. Also, unlike large pore MCM-48, that requires cost-intensive tetraethylorthosilicate as a silica source and the use of a co-surfactant as a pore expander under strong acid conditions.
© 2010 Trade Science Inc. - INDIA

INTRODUCTION

Nanoporous materials have become more and more important in either science or technology. They can be grouped into three classes based on their pore diameter (d): microporous, $d < 2.0$ nm; mesoporous, $2.0 < d < 50$ nm; macroporous, $d > 50$ nm. Among them, mesoporous materials have attracted more attention due to tailoring ability of the pore structure over a wide range, and the potential applications in catalysis, separations, nanoelectronics, sensors, and spacial host materials for substances or reactions[1].

After the first synthesis of the mesoporous silicate molecular sieves denominated M41S by scientists of the Mobil Oil company in 1992[2,3], Huo et al. explained the formation of the mesoporous phases through a cooperative self-organization of charged surfactant micelles and inorganic species[4]. They proposed four synthesis routes based on direct interactions, i.e. S+I‾ or S‾M+I‾, where S and I are the sur-

Full Paper

factant and inorganic species and M are halogenide or alkaline cations. As well as the alkaline and the acidic medium routes, (S^+I^- and $S^+X^-I^+$), mesoporous silica can be prepared by means of the neutral routes $S°I°$ or $N°I°$ through hydrogen bond interactions between non-charged amines ($S°$) or polyethylene oxide ($N°$) surfactants and neutral inorganic species[5,6]. The preparation of mesoporous silica via the neutral route has important advantages over electrostatic routes, because of the easy removal of the surfactant by solvent extraction and the tendency to produce materials with thicker walls and smaller particle sizes.

Most of mesoporous materials are prepared with the micelles formed by cationic surfactants that are used as templates in the formation of mesopores[5-8]. The variation in the sizes and shapes of the templates leads to the formation of mesoporous materials with different pore sizes and structures. Anionic and nonionic surfactants are also employed as templates, but the preparation condition such as the type of silica sources and pH of the synthetic mixtures are considerably different in this case[9,10]. The mesoporous materials that are prepared using anionic surfactants show chiral properties in their pores, and thus, they attract much attention as adsorbents that are useful in the separation of chiral molecules[11,12].

Mesoporous silica synthesized by the use of anionic surfactants were reported by Che et al. (named AMS-n, Anionic surfactant templated mesoporous silica)[13,14]. Che et al. firstly reported the synthesis of highly ordered anionic surfactant templated mesoporous silica (AMS-n) materials using anionic surfactant and co-structure-directing agent (CSDA) through a new S^- $N^{+\sim}I^-$ pathway, where N stands for CSDA. When aminosilane (e.g., 3-aminopropyltrimethoxysilane) or quaternized aminosilane (e.g., *N*-trimethoxylsilylpropyl-*N,N,N*-tri-butylammonium) were used as CSDA, the alkoxysilane site of CSDA co-condensed with inorganic precursors and the ammonium site of CSDA electrostatically interacts with the anionic surfactants to produce well-ordered AMS[14].

This pathway for preparation of mesoporous materials using anionic surfactants is interesting, owing to the novel interaction between the inorganic species and surfactant, as well as the lower cost and toxicity of anionic surfactants than those of the cationic surfactants.

This new synthetic route has been proven a successful way to produce a series of novel mesoporous phases, such as lamellar, hexagonal, cubic and disordered mesostructures[11,13-19].

In this study, the direct synthesis of mesoporous materials is performed by the use of linear alkylbenzene sulphonic acid (LASH) as structure directing agent. The effects of surfactant concentrations on the physical properties and morphology of the mesostructure with a hexagonal phase are observed in detail. All the experiment results are interpreted by the packing parameter which provides a theoretical basis and a useful reference for synthesis of high-performance disordered mesoporous materials in an acid medium.

MATERIALS AND METHODS

Chemicals

Tetraethylorthosilicate (TEOS) was purchased from Sigma Aldrich. Commercial LASH was also used. All the reagents were used as received.

Synthesis pure siliceous MFG-x

In an opened Teflon beaker, 2-8 gm of LASH was added to 90 mL distilled water. The mixture was stirred for 15 min to obtain homogenous solution. 10 gm of TEOS was added portion-wise over 10 min. The mixture was continuously stirred for 4 h at 50 °C. The obtained samples are designated as MFG-x where x is the weight of LASH in mixture solution, e.g. 2 g of LASH: 10 g TEOS, donated MFG-2 and so on. MFG-5 was further synthesized using different water content (40 mL, 90 mL and 160 mL) and donated as MFG-5a-c respectively.

The as synthesized, MFG-x, were transferred into a Teflon bottle and subjected to hydrothermal treatment at 120 °C for 18 h. After the completion of hydrothermal treatment, the solid products were recovered by centrifuge, washed several times with EtOH/H$_2$O (50:50 V/V), dried overnight at 120 °C and calcined at 630 °C for 6 h in air flow to remove the remained organic template. The molar gel composition and structural parameters of, MFG-x, samples prepared at different condition are illustrated in TABLE 1.

TABLE 1 : Molar composition and structural parameters of *MFGs* samples prepared at different condition

Sample	Molar composition	LASH/ H$_2$O (Wt/Wt)	LASH/ TEOS (Wt/Wt)	BET (m^2/g)	Pore volume (CC/g)	Pore diameter [b] (nm)
MFG-2	1 TEOS: 0.128 LASH: 104 H$_2$O	2.2%	16.6%	387	0.32	2.16
MFG-5a	1 TEOS: 0.23 LASH: 46 H$_2$O	11.1%	33.3%	650	0.52	3.58
MFG-5b	1 TEOS: 0.23 LASH: 104 H$_2$O	5.3%	33.3%	584	0.46	3.59
MFG-5c	1 TEOS: 0.23 LASH: 185 H$_2$O	3.0%	33.3%	456	0.33	3.64
MFG-8	1 TEOS: 0.5 LASH: 104 H$_2$O	8.2%	44.4%	523	1.76	12.69

Surface area calculated from BET equation.
Pore volume calculated from the adsorption branch of the isotherm at P/P0 $\approx$ 1.
Pore diameter calculated from the desorption branch of the isotherm according to BJH method.

Characterizations

X-ray diffraction patterns were recorded with a Pan Analytical Model X' Pert Pro, which was equipped with CuKα radiation (λ = 0.1542 nm), Ni-filter and general area detector. The diffractograms were recorded in the 2θ range of 0.5 – 70° with step size of 0.02 Å and a step time of 0.605.

Nitrogen adsorption /desorption isotherms of the synthesized MFG samples were measured on NOVA 3200 system (USA), at -196 °C after degassing at 300 °C and 10-5 mm Hg for 4 h. The BET surface area (SBET) of the investigated samples was calculated from adsorption isotherm data using the BET method. Pore size distribution (PSD) curves were calculated from the desorption branch of the isotherms using the Barrett-Joyner-Halenda (BJH) method.

Scanning Electron Microscopy (SEM) measurement was performed on JEOL JEM electron microscope. SEM was carried out in order to determine the morphology of the sample and the crystal size. Before the measurement, samples were mounted over sample holder (stubs) using double sided tape. The sample was further coated with gold using Sputter Coating System at 10 mbar with current flow, 15 mA.

Transmission electron microscopy (TEM) studies were carried out using a JEOL JEM electron microscope operating at 120 kV. The calcined materials were crushed and dispersed ultrasonically in water at room temperature and then spread onto a perforated carbon–copper microgrid.

RESULTS AND DISCUSSION

The oxide precursors were prepared by the dehydration and polymerization processes of metal alkoxides in water solution, namely sol-gel method. This kind of oxide is stable and favorite to form unique distributed oxide porous structure. Heusch has reported that a dodecyl benzene sulphonic acid mesophase does occur at 40% in water, but has not identified the structure[20]. So, linear alkyl benzene sulphonic acid (LASH) can be used as a structure directing agent for mesoporous silica production. LASH has many advantage over cationic, neutral and polymeric surfactant such as; (1) low cost, (2) good performance, (3) self-catalyst for TEOS, (4) low toxicity and (5) stable at high temperature of hydrothermal treatment.

Commercial LASH composed of a number of different alkyl chain lengths and positional isomers (the benzene ring is substituted on any carbon other than those at either end of the alkyl chain, and a schematic diagram is illustrated in Figure 1. A typical distributional composition is shown in TABLE 2 that gives an average chain length of ≈12.37 carbon atoms and the effective molecular weight is 331 g. There is additional
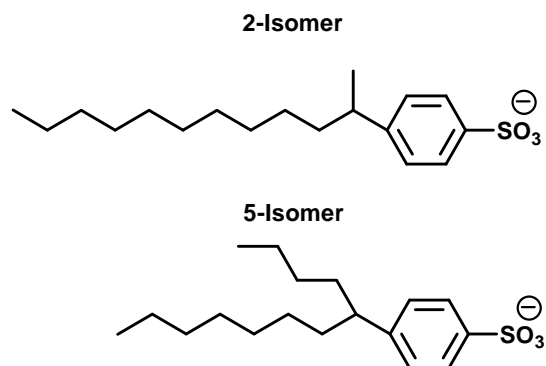
Figure 1 : Typical isomers of alkylbenzene sulphonic acid present in a commercial mixture.

TABLE 2 : Positional isomer distributions (as a wt%) on the different length alkyl chains within typical LASH

Benzene position	Constituent				
	C$_{10}$	C$_{11}$	C$_{12}$	C$_{13}$	C$_{14}$
5	–	–	18.49	13.15	0.08
4	–	–	11.93	18.73	1.72
3	–	6.40	7.35	1.97	8.00
2	7.94	0.03	0.37	1.58	2.25
Total	7.94	6.43	38.14	35.43	12.05

The alkyl chain length here is 12.37 carbons.

Full Paper

sulphuric acid present as an impurity, as well as the un-determined organic matter. Thus, the LASH titrated against known NaOH solutions to establish the final end point, giving an effective molecular weight of 335 g. The true average molecular weight is slightly higher ($\approx$12.6 carbons) due to the presence of H2SO4 which is also neutralized.

Packing constraint considerations

There are three idealized micelle shapes: spheres, rods and discs. Micellar solutions exist only up to a certain concentration of surfactant because the micelles become ordered, forming mesophases at higher con-centrations. The critical packing parameter (g) can be represented as $g = v/lca$ ratio, where v is molecular volume, lc is molecular length, and a is cross-sectional area of the polar head group. This ratio characterizes the spontaneous curvature of the surfactant micelles, and thus describes the real molecular shape of the ac-tual phase. The transitions occur when $a = 3v/lc$ (sphere $\rightarrow$rod) and $a = 2v/lc$ (rod $\rightarrow$disc)[21,22].

The packing parameter g arises from molecular volume Vc and effective length lc, using the following empirical formula[23]:

$$Vc \text{ (Å)}3 = 27.4 + 26.9\ n\ \&\ Lc = 1.5 + 1.265\ n$$

Where n is the number of carbon atoms in the chain. Hence their lc values are $\approx$18.8 Å^2 (taking the benzene ring contribution as 2.8 Å). Whilst only one surfactant chain has to be in the all-*trans* configuration to give the maximum micelle radius, this cannot always be in the same molecule. Hence, we assume that at least $\approx$12% (C_{14} content) of the micelle members must be capable of the maximum L_c value. Thus, the value required is that of the longest 12% LASH. So the estimated aver-age hydrophobic group volume $v = 460$ Å^3. Thus, the shape transitions occur with a=ca. 73 Å^2 (sphere/rod) and a=ca. 49 Å^2 (rod/disc).

Textural properties

XRD, TEM & SEM analysis

The XRD patterns of calcined, MFG-2, MFG-5b and MFG-8, silicas prepared at different LASH/TEOS ratios are illustrated in Figure 2. The patterns showed that worm-like framework mesostructure could be as-sembled from TEOS and LASH. Each sample exhibits a XRD pattern consisting of an intense low angle re-

flection and a weaker, higher angle reflection. These patterns signify the presence of a correlated distribu-tion of framework pores but the lack of a regular pore structure[24]. The pore–pore correlation distance of the calcined samples increases from 8.4 to 8.75 nm upon increasing the LASH/TEOS ratio.
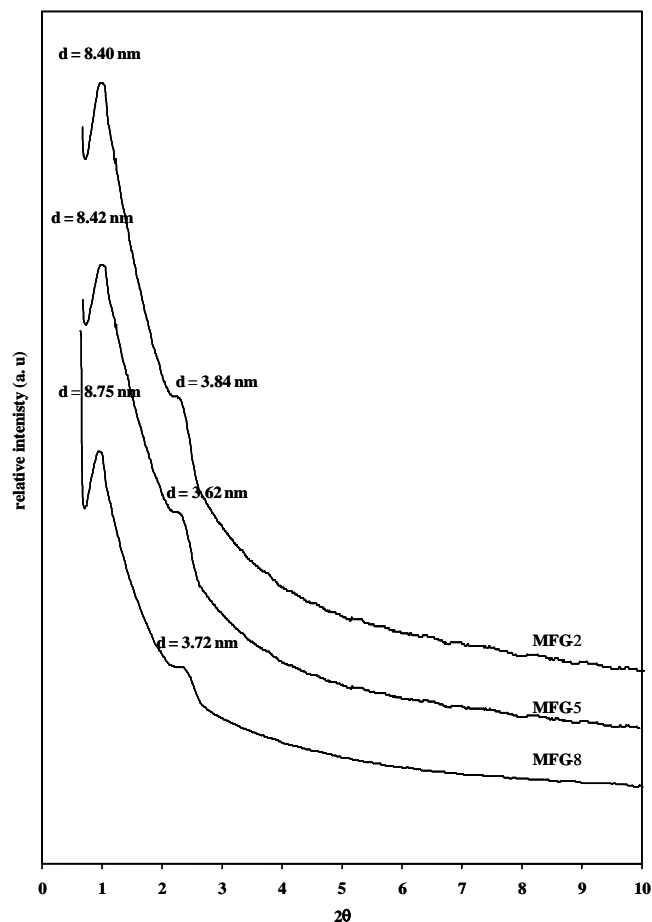

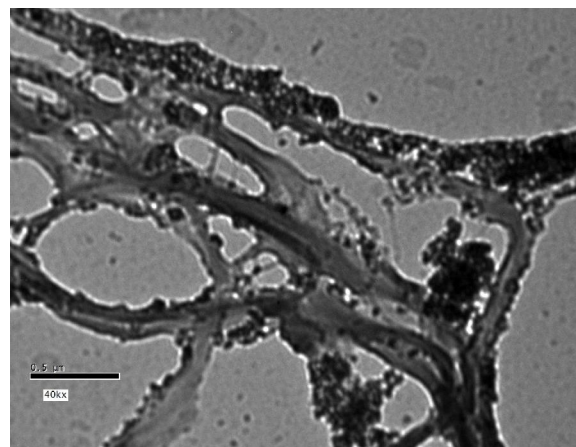**Figure 2 : XRD patterns for calcined MFG-2, MFG-5b and MFG-8 silicate.**
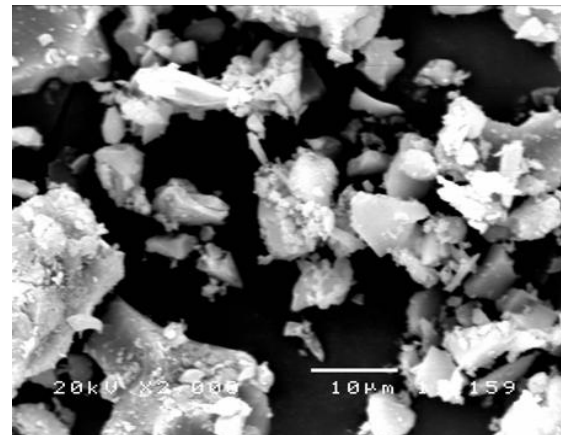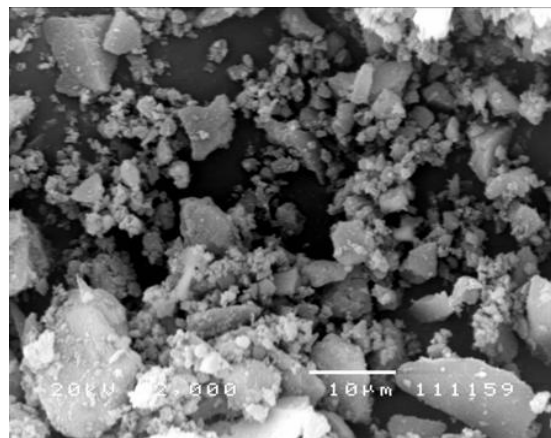

Figure 3 : TEM images of MFG-8 silicas at different mag-nification.

Full Paper

TEM analysis showed that the majority of the pore ordering was not well defined, but that 3-D ordered worm-like or pseudo-hexagonal structure might be inferred (Figure 3), which is consistent with the XRD results. The pore size estimated by TEM analysis is close to that determined from the nitrogen sorption isotherm (TABLE 1).

The SEM images at different magnifications of MFG-x are shown in Figure 4. It is clear that MFGs had a large particle sizes (2-10 µm). In general, the MFGs consist of non-uniform particles with a large external surface area due to the roughness of the surface. Also, the MFGs crystal particles were predominantly plate-like with smooth fine lines on their surface that
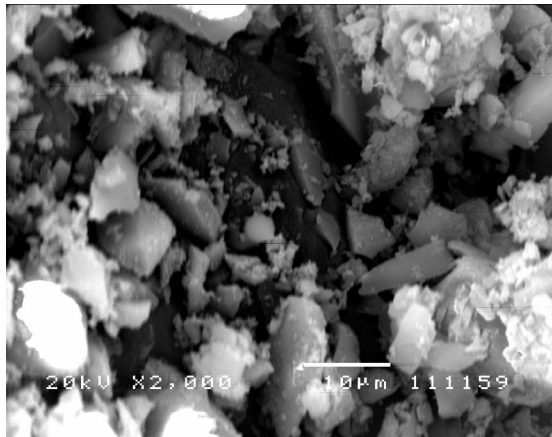
MFG-2
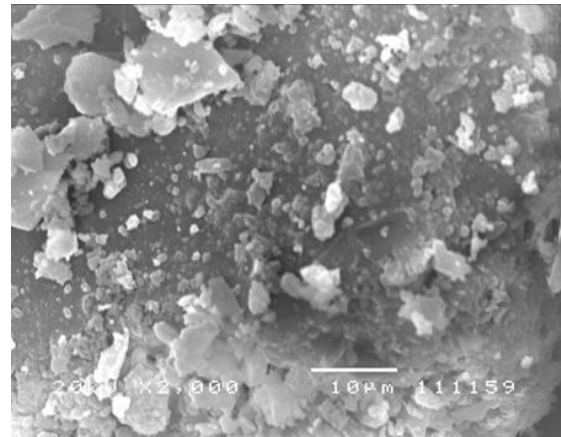
MFG-5a
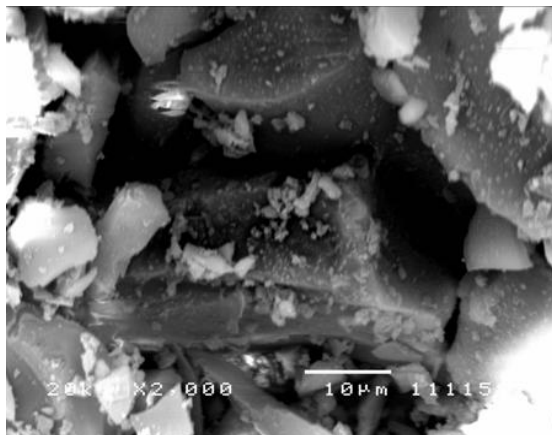
MFG-5b

MFG-5c

MFG-8

Figure 4 : SEM images of different MFG-2, MFG-5-a-c and MFG-8 silicate.

Full Paper

were aligned according to the characteristic morphology. These results indicate that the instant direct-templating method could be applied to form well-known morphological mesoporous silica structures with controlled particle shape and size.

Nitrogen physisorption

Figure 5 illustrates the nitrogen adsorption/desorption isotherms of MFG-2 and MFG-5a-c materials and TABLE 1 shows different textural properties. The isotherm patterns of MFG-2, MFG-5a-c are on the borderline between type I and type IV with a hysteresis loop H1, suggesting the mesostructure of these samples[25], which is consistent with the XRD results. MFG-5a-c showed a higher beginning adsorption capacity than MFG-2, which was reflected in a comparatively larger BET surface areas (650, 584, 456 and 387 m^2g^{-1}) and pore volume (0.52, 0.41, 0.33 and 0.32 cm^3g^{-1}, respectively).
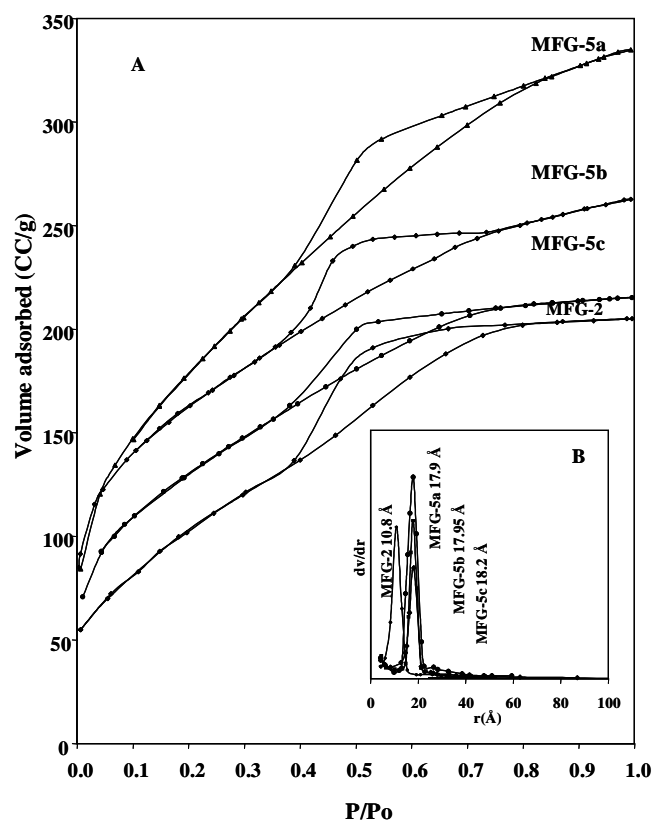

Figure 5 : (A) N$_2$ adsorption–desorption isotherms, (B) pore size distributions for MFG-2, MGF-5a-c silicate.

The isotherm patterns of MFG-8 (Figure 6) showed a Type IV isotherm with a large hysteresis H1 indicating a 3D intersection network of porous structure ac-

cording to IUPAC explanations[27,28], and capillary condensation of N$_2$ occurs at high pressure p/p$_0$ of ca. 0.75-0.9, which indicates the uniformity of the pores. As shown in TABLE 1, the MFG-8, was characterized to be mesoporous with average pore diameter in 12.27 nm and BET surface areas of 525 m^2/g.
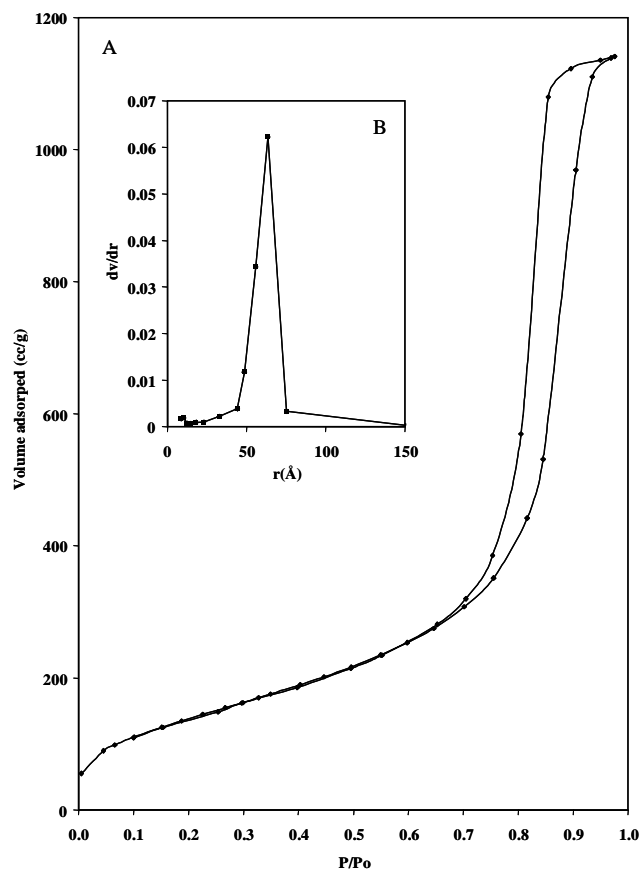

Figure 6 : (A) N$_2$ adsorption–desorption isotherms for MFG-8 silicas. (B) pore size distributions

The new wormhole mesostructures also are comparable in textural properties to 2D hexagonal SBA-15 and large pore cubic MCM-48 derivatives, which exhibit pore sizes in the range 4.7–10.6 nm[28] and 4–12 nm, respectively. However, unlike SBA-15 silicas, which have a hexagonal framework structure wherein 1D cylindrical mesopores are connected by micropores, MFGs mesophases have wormhole framework structures containing interconnected 3D mesopores that can minimize diffusion limitations often encountered in adsorption and chemical catalysis. Large pore MCM-48 also has 3D-connected cylindrical mesopores, but the assembly of these materials requires the use of cost-intensive a pore expanding co-surfactant and swelling agent under strongly acidic reaction conditions. In con-

Full Paper

trast, MFGs wormhole structures are assembled from low-cost a single LASH that has a dual function condition of mesoporous production.

MFG-5a showed high surface area and pore diameter than MFG-2b,c. It is clear that the surfactant concentration and the acidity were decreased with increasing addition amount of H_2O. It is well known that the curvature of the micelle is increased with decreasing concentration of the surfactant, which leads to the mesoporous structure and resulted in increasing mesophase curvature. On the other hand, the less the amount of H_2O, the more the amount of H^+ surrounded the siliceous species, which may catalyze silica condensation. Therefore, the effects of the surfactant concentration may be explained in two ways. One is packing of the surfactant, and the other is charge density matching between the surfactant and silica. Thus, it can be considered that the low addition amount of H_2O favors the formation of higher curvature mesophases with regard the strength of acidity.

The concentration of LASH controls the condensation reaction of siliceous species and the silica condensation causes the positive charge density of the silica network to decrease. To maintain charge matched in the interface, LASH pack to form a high surface curvature so that the transformation to the higher curvature mesophase occurs.

The formation mechanism

Because of LASH considered one of strongest acid, the silica species in solution are positively charged $\equiv SiOH2^+$. The surfactant (S^-)-silica interaction becomes S^-I^+. The amount of electrostatic interaction sites between the anionic surfactant and protonated silica plays an important role to control the mesostructure of the silica[30]. Alkyl chain with a benzene ring at the extremes of the alkyl chain will preferentially form micelles at low concentrations. Firstly, clusters of organic–inorganic composite are formed due to the self-organization between the silica precursors and the surfactant micelles. Secondly, the clusters aggregate to form larger organic/inorganic hybrid[31,32]. At this stage, the surfactant/silica hybrid particle would be soft, i.e., the silica is less crosslinked, and the composite is liquidlike and liable to be shaped.

From TABLE 1, it can be noted that with the in-

crease of the LASH concentration (decreasing pH value), the d_{100} spacing slightly increases and the average pore size increases, indicating that the thickness of the pore wall is reduced. This implies that, at lower pH value, larger amount of interaction sites of the anionic surfactant and hydrated silica induces relatively higher content of surfactant in the surfactant–silica assembly process, The increasing of the pore sizes can also be explained by the more surfactant involved in the co-assembly with the gradual decreasing of the pH values.

It is worthy of special mention that different liquid crystals can formed at high concentration of LASH[33]. At high concentration, LASH particles are included into the liquid crystal, the attractive forces are stronger but the ionic concentration is higher, and swelling is less prevalent. On the other hand, the cationic silica species have ready access to soluble surfactant molecular species and can readily restructure micelle arrays. The role of highly charged cationic polysiliceous species plays an important role in the structure directing, which will control the surfactant geometry through charge density matching and multidentate bonding. So, less anionic surfactants interacted with hydrated silica decrease the local surface curvature energy and leads to the formation of curved morphologies (high surface area).

CONCLUSION

The above results show that large-pore wormhole silica mesostructures are readily prepared through the assembly reactions of linear alkylbenzene sulphonic acid (LASH) without the need for an auxiliary co-surfactant pore expander. The calcined samples of these 3D pore structure exhibit relatively large pore sizes (up to 12.2 nm) and high surface areas (525 m^2g^{-1}) and pore volumes (1.76 cm^3g^{-1}) in comparison to other 3D cylindrical pore systems such as MCM-48. The large interconnected pore systems are ideally suited for the adsorption of large and rigid molecules.

The effect of H_2O/LASH and LASH/TEOS ratios in the synthesis of mesoporous silica has been firstly studied. Lower amount of water is more favorable to form the MFG structure with high curvature. Upon on increasing of LASH concentration, mesostructures of silica with a hollow pore was obtained. Moreover, the

Full Paper

cost effective LASH has a dual function for the assembly of large pore MFG-8 silica without using acidic or basic controlling reactions.

REFERENCES

[1] A.Stein; Adv.Mater., **15**, 763 (**2003**).
[2] C.T.Kresge, M.E.Leonowickz, W.J.Roth, J.S.Beck; Nature, **359**, 710 (**1992**).
[3] J.S.Beck, J.C.Vartuli, W.J.Roth, M.E.Leonowicz, C.T.Kresge, K.D.Schmitt, C.T.W.Chu, D.H.Olson, E.W.Sheppard, S.B.McCullen, J.B.Higgins, J.L.Shlenker; J.Am.Chem.Soc., **114**, 10834 (**1992**).
[4] Q.Huo, D.Margolese, U.Ciesla, D.G.Demuth, P.Feng, T.E.Gier, P.Sieger, A.Firouzi, B.F.Chmelka, F.Schuth, G.D.Stucky; Chem.Mater., **6**, 1176 (**1994**).
[5] P.T.Tanev, T.J.Pinnavia; Science, **267**, 865 (**1995**).
[6] S.A.Bagshaw, E.Prouzet, T.J.Pinnavaia; Science, **269**, 1242 (**1995**).
[7] A.Corma, N.Fornes, M.T.Navarro, J.Perez-Pariente; J.Catal., **148**, 569 (**1994**).
[8] D.Zhao, Q.Huo, J.Feng, B.F.Chmelka, G.D.Stucky; J.Am.Chem.Soc., **120**, 6024 (**1998**).
[9] J.M.Kim, S.K.Kim, R.Ryoo; Chem.Commun., 259 (**1998**).
[10] R.Ryoo, S.H.Joo, J.M.Kim; J.Phys.Chem.B, **103**, 7435 (**1999**).
[11] A.E.Garcia-Bennett, O.Terasaki, S.Che, T.Tatsumi; Chem.Mater., **16**, 813 (**2004**).
[12] S.Che, Z.Liu, T.Ohsuna, K.Sakamoto, O.Terasaki, T.Tatsumi; Nature, **429**, 281 (**2004**).
[13] S.Che, A.E.Garcia-Bennett, T.Yokoi, K.Sakamoto, H.Kunieda, O.Terasaki, T.Tatsumi, Nature Mater., **2**, 801 (**2003**).
[14] A.E.Garcia-Bennett, K.Miyasaka, O.Terasaki, S.Che; Chem.Mater., **16**, 3597 (**2004**).
[15] A.E.Garcia-Bennett, N.Kupferschmidt, Y.Sakamoto, S.Che, O.Terasaki; Angew.Chem. Int.Ed., **44**, 5317 (**2005**).
[16] A.E.Garcia-Bennett, K.Lund, O.Terasaki; Angew. Chem.Int.Ed., **45**, 2434 (**2006**).
[17] C.Gao, Y.Sakamoto, K.Sakamoto, O.Terasaki, S.Che; Angew.Chem.Int.Ed., **45**, 4295 (**2006**).
[18] X.Wu, H.Jin, Z.Liu, T.Ohsuna, O.Terasaki, K.Sakamoto, S.Che; Chem.Mater., **18**, 241 (**2006**).
[19] C.Gao, H.Qiu, W.Zeng, Y.Sakamoto, O.Terasaki, K.Sakamoto, Q.Chen, S.Che; Chem.Mater., **18**, 3904 (**2006**).
[20] R.Heusch, Tr.Mezhdunar.Kongr.Poverkhn.Akt. Veshchestvam, 7th Ed., **2(2)**, 911-939, (**1976**).
[21] H.Kunieda, M.Horri, M.Koyama, K.Sakamoto; J.Colloid Interface Sci., **236**, 78 (**2001**).
[22] J.Lee, J.Kim, T.Hyeon; Chem.Commun., 1138 (**2003**).
[23] H.P.Lin, Y.R.Cheng, C.Y.Mou; J.Mater.Chem., **9**, 1197 (**1999**).
[24] I.Park, T.J.Pinnavaia; Micropor.Mesopor.Mater., **118**, 239 (**2009**).
[25] D.Jiang, J.Gao, J.Li, Q.Yang; C.Li.Micropor.Mesopor.Mater., **113**, 385 (**2008**).
[26] K.S.W.Sing, D.H.Everett, R.A.W.Haul, L.Moscou, R.A.Pierotti, J.Rouquerol, T.Siemieniewska; Pure Appl.Chem., **57**, 603 (**1985**).
[27] J.Rouquerol, D.Avnir, C.W.Fairbridge, D.H.Everett, J.H.Haynes, N.Pericone, J.D.F.Ramsay, K.S.W.Sing, K.K.Unger; Pure Appl.Chem., **66**, 1739 (**1994**).
[28] J.S.Lettow, Y.J.Han, P.Schmidt-Winkel, P.Yang, D.Zhao, G.D.Stucky, J.Y.Ying; Langmuir., **16**, 8291 (**2000**).
[29] M.V.Landau, L.Vradman, X.Wang, L.Titleman; Micropor.Mesopor.Mater., **78**, 117 (**2005**).
[30] C.Gao, H.Qiu, W.Zeng, Y.Sakamoto, O.Terasaki, K.Sakamoto, Q.Chen, S.Che; Chem.Mater., **18**, 3904 (**2006**).
[31] A.Galarneau, F.Di Renzo, F.Fajula, L.Mollo, B.Fubini, M.F.Ottaviani; J.Colloid Interface Sci., **201**, 105 (**1998**).
[32] J.Zhang, H.Zimmermann, Z.Luz, D.Goldfarb; Stud.Surf.Sci.Catal., **117**, 535 (**1998**).
[33] J.A.Stewart, A.Saiani, A.Bayly, G.J.T.Tiddy; Colloids and Surfaces A: Physicochem.Eng.Aspects, **338**, 155 (**2009**).